Methodology to Analyse Handling Qualities under Force Gradient Transitions of an Active Sidestick

Eduard Rauer*
Technische Universität Berlin
Institute for Aeronautics and Astronautics
Department of Flight Mechanics, Flight Control and Aeroelasticity
Marchstraße 12, 10587 Berlin, Germany

In recent years active sidesticks have been introduced in civil aircraft enabling more intuitive force-feedback, amongst other improvements. But mode degradations or mechanical failures can cause sudden transitions in the force-deflection gradient. During manual control, such an event can lead to overcontrol by the pilot and into a PIO. A methodology is developed to investigate the impact of these events on pilot-vehicle system dynamics. Tracking tasks are designed to repeatedly elicit pilot reactions comparable to those of sudden and unexpected transitions. First simulator tests proved the methodology to be effective in surprising the pilot and preventing memorisation. They reveal that transitions have a greater impact when gradients decrease and pilots are well adapted.

Nomenclature

FCS	Flight Control System	δ	Inceptor deflection angle
IAS	Indicated Airspeed	ζ	Damping ratio
LVDT	Linear Variable Differential Transformer	ω_0	Resonance frequency
PFD	Primary Flight Display	η	Elevator deflection angle
PIO	Pilot in-the-loop Oscillation	Θ	Pitch attitude angle
PSD	Power Spectrum Density	K_i	Static gains
PVS	Pilot-Vehicle System	k_i	Non-dimensional force-deflection gradients

I. Introduction

Force-feel characteristics of mechanical flight controls with reversible linkages are influenced by aerodynamic effects. The most important among them is the proportional dependency of force-deflection gradient from dynamic pressure. At high indicated airspeeds (tantamount to high dynamic pressure) the same inceptor deflection thus requires a higher force than at low IAS. Fly-by-Wire Flight Control Systems with passive inceptors eliminate this relationship as the force-deflection gradient is determined by mechanical springs and dampers and therefore independent of IAS.

Compared to their passive counterparts, active inceptors in addition feature electric torque motors that provide position control and variable force feedback. They are hence capable of replicating desirable features of traditional flight control concepts like tactile command feedback from the autopilot or the second pilot [1]. Furthermore, the force-deflection gradient can be varied according. Active sidesticks with these capabilities are currently in service in military aircraft, e.g. F-35 and Embraer KC-390, and civil aircraft, Gulfstream G500 and MC-21 [2].

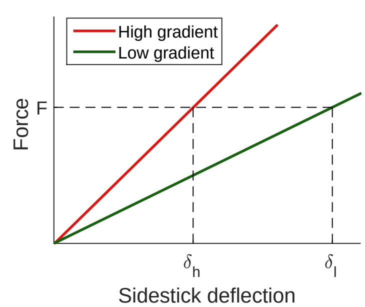

Figure 1. Force gradient transition

In cases of FCS mode degradations or mechanical failures of the active sidestick, sudden changes of the force-deflection gradient can happen suddenly or inadverntenly. In the example in Figure 1, the high force-deflection gradient corresponds to flight regimes with high IAS that impedes involuntary large deflections that could exceed the aircraft's structural limits. The 50% lower gradient corresponds to low IAS and enables more agile maneuvers in regions of the flight envelope where full deflections do not cause dangerous load factors. In the first moment after an unexpected and sudden gradient transition from high to low, the pilot does not immediately readapt the force of his inputs. Under this circum-

*Former M.Sc. Aeronautics and Astronautics Engineering student, `eduard.rauer@hotmail.com`

stance, the gradient reduction doubles the sidestick deflection unwantedly from δ_h to δ_l. At high IAS the resulting overcontrol can lead to a PIO with dangerous of even fatal load factors, as reported in [3].

This paper describes a methodology to determine the impact of abrupt transitions of the force-deflection gradient on pilot-vehicle system dynamics in pilot tests. The developed methodology is applied to investigate PIO-occurrence in single-axis pitch tracking tasks in a fixed-base simulator. Pilots fly the tests with an active sidestick that replicates three force deflection gradients. Six gradient transissions are possible between them. The special requirement for the simulator tests is to reconcile an apparent contradiction: the systematic repetition of a situation intended to surprise the pilot at every time. The methodology is thereafter verified in simulator tests and the results are evaluated.

II. Apparatus

The Handling Qualities Investigation Test Station at the Department of Flight Mechanics, Flight Control and Aeroelasticity (FMRA), depicted on the left image of Figure 2, is built around the active sidestick (1). The sidestick was built for research purposes. It houses an LVDT, strain gauge, spring-damper, and torque motor in pitch and roll axes to measure displacement, force and confer the sidestick basic and variable force-feel (gradient and damping) respectively.

The simulation of aircraft equations of motion with the definition of force-feel variables runs at 50 Hz on computer (2). Computer (3) is dedicated to the data interface between simulation computer and sidestick power electronics (4). The power electronics send the desired force-feel characteristics to the sidestick and receive the pilot's commanded inputs. Each computer has its corrresponding input and output devices on the desk. The display computer (5) generates a PFD on the right monitor.

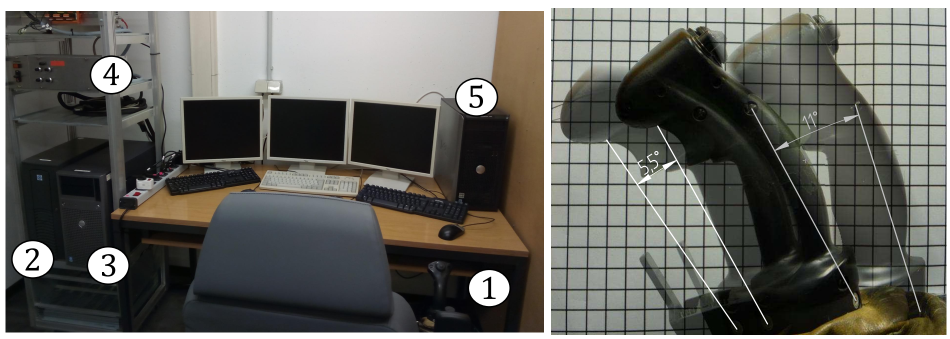

Figure 2. Handling qualities test station (left) and close-up active sidestick deflections (right)

The active sidestick can be mechanised as a force or deflection sensing inceptor. The former uses pilot force directly as input to the FCS. But this principle has often yielded unsatisfactory results [4]. With a deflection sensing inceptor, pilot force is first transformed into a deflection through the force-feel system and then used as input [5]. This inceptor layout is the most commonly used and therefore also applied for these tests.

The sidestick's force-deflection gradient and damping are set through non-dimensional values between 0 and 1. These values guard no direct relation with the physical quantity they represent. For the simulator tests the damping is constant at 0.3 and The force-deflection gradient k is varied among three values: k_1=0; k_2=0.3; and k_3=0.7.

Continuos lines in Figure 3 show force-deflection curves with -6.7 N and 5.0 N breakout forces measured in previous internal studies. For the present investigation, constant gradients for the entire deflection range are approximated (values written into Figure 3). The aft (positive) deflection angle was found to be erroneous because the LVDT reached its maximum output voltage before the physical hardstop and did not measure the last portion of the rearward travel. This explains the vertical peaks of the three curves at 9.9°. While the force measurements continue increasing, deflection measurement remains constant. Figure 2 depicts the corrected deflections of -5.5° – 11°.

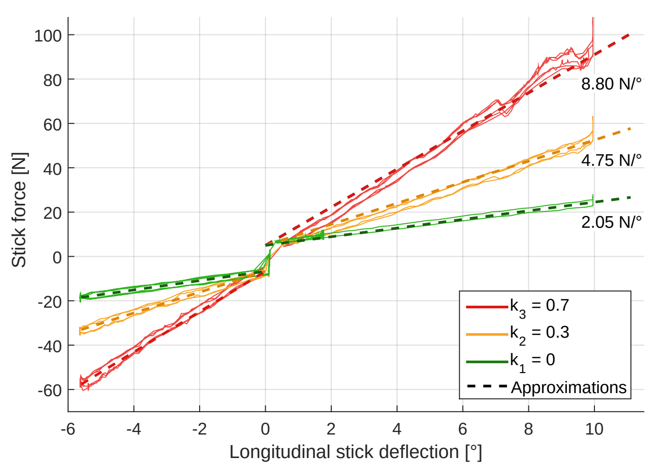

Figure 3. Approximated and measured force-deflection curves

Sidestick dynamics are modelled as a second order spring-mass-damper with the general form:

$$Y_{2^{nd}O} = \frac{K\,\omega_0^2}{s^2 + 2\,\zeta\,\omega_0\,s + \omega_0^2}\,. \qquad (1)$$

The input to the sidestick transfer function $Y_{\delta,F_{st}}$ is the pilot force exerted at the stick F_{st} and the output is angular deflection δ. Static gain $K_{st,i}$ corresponds to the inverse of the three force-deflection gradients from Figure 3:

$$K_{st,1} = 2.05^{-1} = 0.49\ °/N \qquad K_{st,2} = 4.75^{-1} = 0.21\ °/N \qquad K_{st,3} = 8.80^{-1} = 0.11\ °/N. \tag{2}$$

Identification of sidestick dynamics in [6] yielded:

$$\omega_{0,st} = 30.6\, rad/s \qquad \zeta_{st} = 0.78. \tag{3}$$

III. Analysis of the tested aircraft dynamics and transitions

The simulator tests are flown with two longitudinal aircraft dynamics to determine if differences in their behaviour has an effect on PVS dynamics after force-deflection gradient transitions. It was established that the handling qualities rating of both dynamics should differ noticeably, approximately by one level.

During the pitch tracking task, the pilot closes the loop around Θ. All the elements between inceptor and simulation module are controlled by the pilot and threfore have to be taken into account for handling qualities analysis.

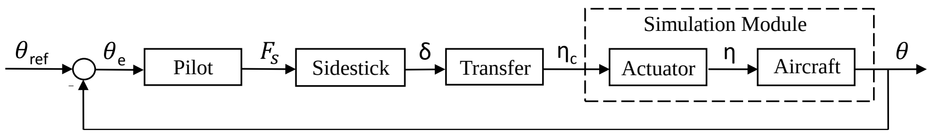

Figure 4. Control loop closed around pilot and controlled element

The resulting "controlled element", is depicted in Figure 4. It is composed by the transfer functions of the active sidestick's feel system $Y_{\delta,F_{st}}$, computing time and transmission delays (joined under the term "Transfer") $Y_{\eta_c\delta}$ and the simulated components: second order actuator $Y_{\eta\eta_c}$, and FCS-delay with fourth order aircraft dynamics $Y_{\Theta\eta}$. All the transfer functions contained in Equation 4, except $Y_{\Theta\eta}$, are the same for both controlled elements.

$$Y_{\Theta F_{st}} = Y_{\Theta\eta} \cdot Y_{\eta\eta_c} \cdot Y_{\eta_c\delta} \cdot Y_{\delta,F_{st}} \tag{4}$$

The Sidestick dynamics were already characterised in Equations 2 and 3. The three different gains from the sidestick gradients do not influence the handling qualities rating and do not require to be considered separately. Transfer delay τ_{trans} is the time it takes for a sidestick deflection δ to be trasnferred to the simulation module as a commanded elevator deflection η_c. Its approximation is based on discretisation times of the involved components. Data transfer from the interface to the simulation module is clocked at 100 Hz (0.01 seconds per time step). As the simulation runs at 50 Hz, 0.02 seconds elapse between two samples. In the most unfavourable case, a pilot input can thus take up to 0.03 seconds until becoming effective.

$$Y_{\eta_c\delta} = e^{-\tau_{trans}} = e^{-0,03} \tag{5}$$

The second order actuator is also modelled as a second order as in Equation 1 with:

$$K_{act} = 0.7 \qquad \omega_{0,act} = 45\, rad/s \qquad \zeta_{act} = 0.7 \tag{6}$$

The simulated aircraft is different for the two controlled elements. They are both Class II aircraft in the landing approach configuration from a database at FMRA. They are composed of short period and phugoid dynamics and of a delay τ_{FCS} that represents the FCS. It is the most distinct difference between the configurations, which is why the first one characterised by:

$$\omega_{0,SP} = 2.19\, rad/s \quad \zeta_{SP} = 0.51 \quad \omega_{0,PH} = 0.15\, rad/s \quad \zeta_{PH} = 0.059 \quad \tau_{FCS} = 0.03\, s \tag{7}$$

is called $D_{\tau_{short}}$ and the second is called $D_{\tau_{long}}$

$$\omega_{0,SP} = 1.89\, rad/s \quad \zeta_{SP} = 0.48 \quad \omega_{0,PH} = 0.17\, rad/s \quad \zeta_{PH} = 0.145 \quad \tau_{FCS} = 0.109\, s. \tag{8}$$

A set of requirements is established to select the appropriate criteria to evaluate the handling qualities of the above described controlled elements.

- **Acceleration:** Criteria relying on acceleration cues are excluded . The fixed base simulator does not influence pilot perception through accelerations.
- **Class II:** Criterion premisses should be valid for Class II transport aircraft performing a Category C task (a landing approach for the present case).

- **Proportionate effort:** The effort to apply one criterion should be proportionate and justified by the findings it is expected to reveal.
- **PIO predictor:** Criteria should be a good predictor of PIO and its severity. The criteria should, as an ensemble, consider as many PIO influence factors as possible.

For this reasons the reason fell upon the Neal-Smith Criterion, Bandwidth Criterion, and Gibsond's Dropback and Frequenc Response Shape Template. The Neal-Smith Criterion is adapted to the demands of a Cat. C task of a Class II aircraft with a bandwidth of 1.5 rad/s and 0.25 seconds pilot delay. To adapt the Bandwidth Criterion the revised boundaries from the study[7] are used.

Criterion	Neal-Smith	Bandwidth	Dropback	Template
$D_{\tau_{short}}$	1	1	1	3
$D_{\tau_{long}}$	1-2	2	1	-

Table 2. Handling Qualites ratings of both controlled elements

The results in Table 2 include the whole controlled element, although the respective row is only labelled with the name of the simulated aircraft dynamics. Neal-Smith and Bandwidth criteria evaluate both controlled elements as being approximately one rating level apart from each other. According to the Dropback Criterion definition by [8] both dynamics offer Level 1 qualities according to Gibson's original boundaries in [9] both will have an abrubt tendency to bobble. Gibson's Template detects deficient damping at -180° phase and predicts Level 3 qualities for the controlled element around dynamic $D_{\tau_{short}}$ and even worse for $D_{\tau_{long}}$.

IV. Test methodology

Transition (k)	0 → 0.7	0 → 0.3	0.3 → 0.7	0.7 → 0.3	0.3 → 0	0.7 → 0
Name	T+3	T+2	T+1	T-1	T-2	T-3
Factor (dec)	0.23	0.43	0.54	1.85	2.32	4.30
Factor (dB)	-12.7	-7.3	-5.4	5.4	7.3	12.7

Table 3. Open-loop gain factors for force-deflection gradient transitions

The methodology described in this section is designed to be verified by pilots without previous testing experience. It therefore abstains from the use of rating scales and includes five test runs to acquire the proper flying technique. In case the methidology is adapted for experienced test pilots, rating scales should be included.

The main objective of the simulator tests is the investigation of transitions between the three force-deflection gradients. The six transitions are identified in Table 3 with the two involved non-dimensional force-deflection gradients k and a name. They are in order of increasibg open-loop gain variation. For the first three transitions with positive sign in their name, the sidestick gradient increases (open-loop gain decreases). The last three have a negative sign because the sidestick gradient shifts towards lower values (open-loop gain increases). The cypher following the sign quantifies the magnitude of gradient variation. For example T+3 transitions from the lowest gradient $k_1 = 0$ to the highest gradient $k_3 = 0.7$. Since the force-deflection gradient increases from 2.05 to 8.80 °/N, the open-loop gain reduces by a factor of 0.23 or -12.7 dB. On the outer columns the absolute value of the factor is higher (± 3) than in the central columns (± 1).

$D_{\tau_{short}}$	$D_{\tau_{long}}$	Gradients
21	24	$K_{st,1}$
22	25	$K_{st,3}$
23	26	$K_{st,3}$
31	37	T+2
32	38	T+3
33	39	T+1
34	40	T-2
35	41	T-3
36	42	T-1
51	55	T+1, T-3
52	56	T+1, T-1
53	57	T-2, T+3
54	58	T-3, T+2

Table 4. Gradients and nomenclature of evaluated test runs

The transitions act in the following way: While the pilot is flying the task, the force-deflection gradient changes abruptly to a stiffer or softer setting according to Table 3. The aim to surprise the pilot so he is unable to predict the transition or prepare for it. In this sense especially the first transition bears the highest potential because habituation will mild the effect of the subsequent transitions. So in order to make the remaining test runs equally unpredictable, tests sessions include many variations. The first variation possibility is the number of transitions included in a test run: none, one or two. Various reference functions and randomisation of the test order for each pilot are also employed to compensate learning effects, fatigue and avoid monotony.

A nomenclature is established to identify the test runs. Runs number 1-3 are trainings to adapt to the three force-deflection gradients. Numbers 4-8 prepare the pilot in the HQDT technique. Test runs 11-13 and 14-16 are flown before the evaluated test runs to adapt the pilot to the three force-deflection gradients combined with both aircraft dynamics. There are 26 evaluated test runs, listed in Table 4. Test runs 21-26 have no transition (used to infer the pilot's performance in undisturbed conditions), 31-42 have one transition and 51-58 two. Test runs with two transitions allow making a better use of the run time and adding asurprising potential when the pilot is starting to get used to assume that each run will have one transition. Therfore test runs with two transitions did not appeared earlier than fourth. The first column in Table 4 corresponds to test runs with dynamic $D_{\tau_{short}}$, the second to $D_{\tau_{long}}$.

A. Handling Qualities During Tracking

For high-precision high-gain tasks, like approaches in turbulent conditions, low fuel or other emergencies, pilot behaviour can shift towards high-frequent, large-amplitude inputs. To test Handling Qualities and PIO-proneness for these conditions, pilots are required to fly with high bandwidth and gain [10]. Developed to evaluate "Handling Qualities During Tracking", this technique is conveniently abbreviated as HQDT. Tracking the reference function with the HQDT technique exposes flaws that the aircraft would otherwise only unveil under exceptional operational conditions. As flying with this technique is unnatural, pilots receive a training prior to the tests that follows the HQDT build-up philosophy. Input bandwidth is increased first, then the input amplitude. This is done by varying frequency content and amplitudes of the reference function.

Instructions for the HQDT technique, stating the importance of aggressive command inputs, are included in the briefing. Maximum error values for the training test runs motivate the pilots to maintain a high gain. Boxes around the aircraft nose symbol on the PFD in Figure 5, akin to a gun pipper, visualise the error. The amber coloured box delimits $\pm 2°$ error and the red one $\pm 4°$. The pilot should keep the flight director inside the amber limits when the reference pitch angle increment is small. When the reference function varies at a high rate, the flight director is allowed to escape into the red box and has to be brought back into the amber limits as quickly as possible.

B. Briefing and questionnaire

The importance of preparing the pilots for the tests is lined out in [11]. An important factor in briefings is to give the pilots the necessary information to carry out the tasks as required without revealing information from which they could deduce potential outcomes beforehand. This is called pilot naiveté and means, that there are details, e.g. on configuration or aircraft dynamics, that the pilot should ignore to ensure his perception is unbiased.

A briefing was sent to the pilots two days prior to the test day. It contains test background, a description of the test structure, the required HQDT technique, and the sidestick characteristics. The written briefing explains the three force-deflection gradients but not that transitions between them will occur. Surprise is assumed to be a main contributor to torce-deflection gradient transitions effectiveness. But if the pilot is not warned about their presence, he could back off from the controls thinking something broke, hence spoiling the test run. This is the reason why the transitions were revealed to the pilot during the verbal briefing before the tests to avoid that possible misconceptions could persist over days or that he could plan how to tackle the event. However, to give as little information as necessary, details on how the transitions develop are kept to a minimum and left for the pilot to discover. As the test session goes on, the pilot learns what to expect.

Revealing as little information as possible on the transitions and achieving meaningful data was also the philosophy behind the questionnaire after every test run. Its first four questions have a hierarchical order, each one aimed at revealing further details of the event, how it had affected the pilot and his adaption. Only an affirmative answer of the previous question leads on to the next one, where more details are enquired. This structure prevents that the questions give away information about the transitions that the pilot has not yet found out on its own. The questions are phrased in an open way, avoiding terminology that may bias the answers.

1. **Question 1:** Did you notice a transition? Did it disrupt you?
2. **Question 2:** What was the reason for the disruption?
3. **Question 3:** Did you perform better before or after the transition?
4. **Question 4:** Did you change your behaviour to regain control?

Apart from answering the questions, the pilots are also encouraged to comment extensively on their subjective performance, predictability of the task or explaining any special events. If the evolution of the test run demanded it, the questions were adapted to address special events. A fifth question served to determine the trend in workload and fatigue over a test session. With a simple scale, 1 being the lowest workload and 4 the highest, pilots estimate the time they could keep up the same performance. 1 means, they could keep up the performance level for a flight of an hour, 2 for a couple of minutes (between 5-10). A workload rated as 3 means, that their performance would decrease shortly after the test run and 4, that it already decreased during the test run.

C. Unpredictability through various reference functions

For the present simulator tests compensatory behaviour in the pitch axis is implemented through the PFD depicted in Figure 5, where the pilots have to track the green flight director bar with the aircraft nose symbol. But the artificial horizon in the PFD allows the pilots to see the response to their inputs and build a mental model of the aircraft. In control terms, they introduce a feed-forward path and their behaviour turns from compensatory to pursuit. Despite this difference, the crossover pilot model is still valid for this type of pilot behaviour [12]. Speed and altitude are held fixed to help the pilot focus solely on pitch attitude.

To obtain a reference function that is intransparent and unpredictable to the pilot, the flight director is driven with a random-appearing sum of j=1-10 sinusoids $r(t)$. The pilot bandwidth while tracking the flight director should be comparable to that of a landing approach task of a Class II aircraft, established as 1.5 rad/s.

$$r(t) = \sum_{j=1}^{n} A_j sin\,(\omega_j t). \tag{9}$$

An appropriate power spectrum was developed by Damveld in [13] and is represented in Table 5. When inserted into Equation 9 it yields a function of 108 seconds period intended for test runs of this duration. Its amplitude in degrees drives the flight director in the PFD.

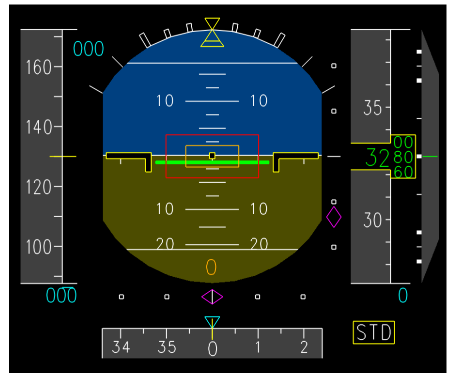

Figure 5. PFD used for tracking tasks

But the duration of the present test runs was reduced to 80 seconds. It was suspected that 108-second long test runs would cause the pilots frustration and too much fatigue after an entire session. The main interest lays on the effects of a transition, estimated to last 5-10 seconds. Test runs of too much duration would ofuscate the pilot's memory on an event that happened almost two minutes ago and rather impede accurate comments at the end of the test run.

j	Frequency ω_j (rad/s)	Magnitude A_j (°)
1	0.175	6.45
2	0.291	6.45
3	0.465	6.45
4	0.640	6.45
5	0.989	6.45
6	1.51	6.45
7	2.50	0.46
8	4.13	0.46
9	7.62	0.46
10	13.56	0.46

Table 5. Reference function for evaluated test runs based on [13]

To prevent the pilot from memorising parts of the reference function even until the last of the 26 test runs, two measures were taken to modify the original function. The first is extracting three different 80-second segments from the original by setting off their origin 7.3; 38.8; and 95.5 seconds from the original. The offsets are chosen in such a manner, that the beginning of the three segments is gentle and the pilot is not blindsided at the beginning. As a second measure, the symmetrical counterparts of the three reference functions (amplitudes of opposite sign) are also used. Figure 6 (left) examplifies the procedure for the first offset.

Not only the reference function has to remain unpredictable to the pilot, also the moments, at which transitions happen. If the pilot is able to recognise a pattern in the reference function that always precedes the force-deflection gradient transition, he can prepare himself raising his level of attention or grip force. If the transitions are programmed at a constant time he could do likewise. Four possible transition moments are thus defined. They are evenly spread over the 80 seconds in such a way that the first is long enough after the beginning and the last leaves sufficient time for the possible pilot reaction. It is not sensible to trigger the transitions manually, since the test conductor is in the pilot's sight.

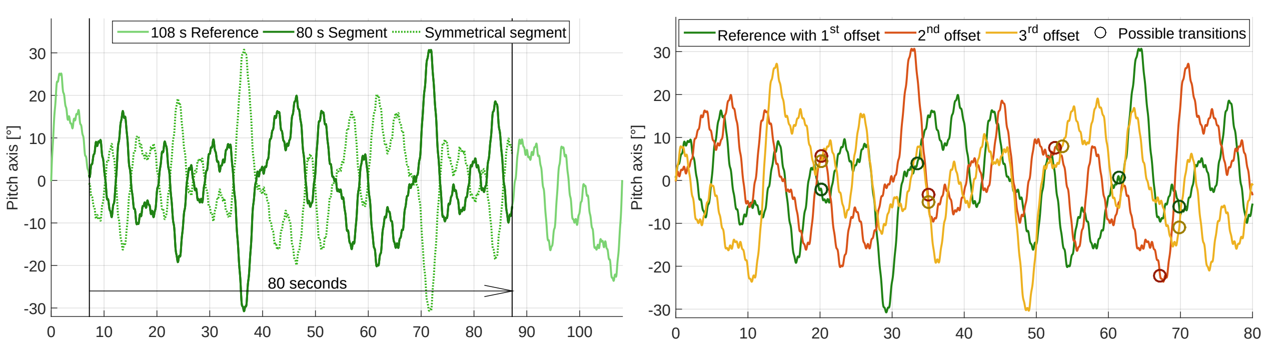

Figure 6. Extractrion of reference function with 1^{st} offset from 108-seconds long function (left), all three with transition moments (right)

Figure 6 (right) shows the four possible transition moments for each one of the reference functions. They were placed in regions of smaller and larger deflections, with smaller and larger pitch rates, i.e. regions witch different expected sidestick amplitudes and travel speeds.

D. Randomisation

It is expected that the pilots' performance and adaption improves as the session progresses because they learn to deal with the dynamics and transitions. These effects are cancelled through randomisation: arranging test sessions in different order. Evaluated test runs are flown in two blocks of 13 runs, one block for each dynamic. Three pilots fly Dynamic $D_{\tau_{short}}$ first and $D_{\tau_{long}}$ afterwards. The other three pilots in the inverse order.

Pilot	First turn	Second turn
Pilot 1	Block 1	*Block 3*
Pilot 2	*Block 1*	Block 3
Pilot 3	Block 2	*Block 1*
Pilot 4	*Block 2*	Block 1
Pilot 5	Block 3	*Block 2*
Pilot 6	*Block 3*	Block 2

Table 6. Randomisation of test sessions. Dynamic $D_{\tau_{short}}$ in normal font, $D_{\tau_{long}}$ in italic font

To define each test session, two out of six blocks are selected. The six blocks, each one with 13 runs, are derived from Block 1, 2, and 3. Block 1 begins with transitions of increasing gradient (T+1, T+2, and T+3) and Block 2 with transitions of decreasing gradient (T-1, T-2, and T-3). Block 3 is mixed. The test runs from the first column of Table 4 (dynamic $D_{\tau_{short}}$) are arranged in three blocks accoring to these rules. Three more blocks originate when the equivalent test runs of dynamic $D_{\tau_{long}}$, i.e. second column but same row, are arrangd in the same order. Tthe first test runs of the six blocks cover the six different the transitions from Table 3. Test runs with two transitions (51-58) do not appear before the fourth run. The average position of test runs is balanced out between the blocks so they are all effected equally by learning effects or fatigue.

After the first block, pilots fly the second dynamic with a different block number (see Table 6). This allows comparing trends in the performances of two pilots who flew the same block in different positions, where learning effects or fatigue play a different role.

V. Test Evaluation

A test campaign was planned based on the methodology from Section IV to verify its applicability and evaluation approaches. Five pilots were recruited from among fellow students. They had different backgrounds and experiences, summarised in Table 7, which influenced their flying techniques. The pilot planned as Pilot 4 could not take part in the test campaign. Pilot 2 came to the test session after a full workday and Pilot 5 was not well rested the morning of his test session. This has an effect on their performance and endurance. The test sessions were structured as described in Table 6. Pilots 2 and 3 flew 4 test runs less in their second block due to fatigue and time constraints respectively.

A. Chracterisation of pilot behaviour

To evaluate the pilot reaction to force-deflection gradients and their flying technique, especially the implementation of an aggressive HQDT control behaviour, the following variables are analysed:

- **Pilot bandwidth** measuring the highest frequency until which the pilot reacts to inputs. For HQDT test data, bandwidth is the highest frequency at which the PSD of pilot inputs is at least an order of magnitude below the peak value. Bandwidth frequency is defined relative to the global maximum in the PSD. Therefore pilots with similar bandwidth frequencies can have very different input amplitude levels.
- **Deviation of error** σ over a test run as a measure of pilot performance. It is equivalent to the RMS of error. For n discrete and equally weighted values of error Θ_e, it is computed as

$$\sigma = \sqrt{\sigma^2} = \sqrt{\frac{1}{n}\sum_{i=1}^{n} {\Theta_{e,i}}^2}. \tag{10}$$

- **Time shift of reference function** measures the delay of aircraft response with respect to the reference function. It is used as an indicator for the pilot's caution or confidence to react quickly. To obtain it, the reference function time series is shifted forward (towards higher times) until the error, cumulated over the test run, is minimal.
- **Physical effort** is quantified with deviation or RMS of pilot force measured as a non-dimensional variable by the active sidestick over a test run. Sidestick force depends on deflection and force-deflection gradient. So even at full deflections with low gradient (k_1), pilot force cannot reach the values of high gradients (k_3).

Pilot	Experience	Remarks
Pilot 1	Extensive simulator experience	
Pilot 2	80 h on glider 150 h on motor glider 70 h on single engine piston	Aerobatics training
Pilot 3	400 h on fighter jet (incl. trainer) 1350 h on military transport	No sidestick experience
Pilot 5	750 h on ultralight aircraft 80 h on motor glider 40 h on single engine piston	
Pilot 6	100 h on single engine piston	Simulator experience

Table 7. Pilot experience and qualifications

Test run errors are plotted in Figure 7 (left) in chronological order. Except Pilot 3, the other four pilots' performances improve until they stabilise between test run 7 and 14. These initial test runs are hence influenced by improving adaption.

Figure 7 (right) represents physical workload in the same manner. The limit between blocks is easily identifiable between test runs 13 and 14. Workload levels for pilots who flew dynamic $D_{\tau_{short}}$ in the first block increase (Pilots 1,3 and 5), while the inverse applies to Pilots 2 and 6. The higher physical workload for $D_{\tau_{long}}$ confirms its less benevolent handling qualities obtained in Section III. Subjective workload of Pilots 1, 2, and 5 coincides with it. Pilots 3 and 6 however subjectively perceived a lower workload for dynamic $D_{\tau_{long}}$.

Pilots 1 and 6, had overall similar error values and flew $D_{\tau_{long}}$ with Block 3 (see Table 6). The difference was that Pilot 6 flew it in first, Pilot 1 in second place. In 11 out of 13 test runs with this dynamic, Pilot 1 flew with less error. This indicates that the practice acquired during the first block was beneficial to fly the other dynamic in the second block. Overall lower errors for all pilots in the second half confirms this The high error of Pilot 6 in test run 21, a point where the pilot had worked out a strategy for the tracking, was caused by intructions of the author to stay aggressive.

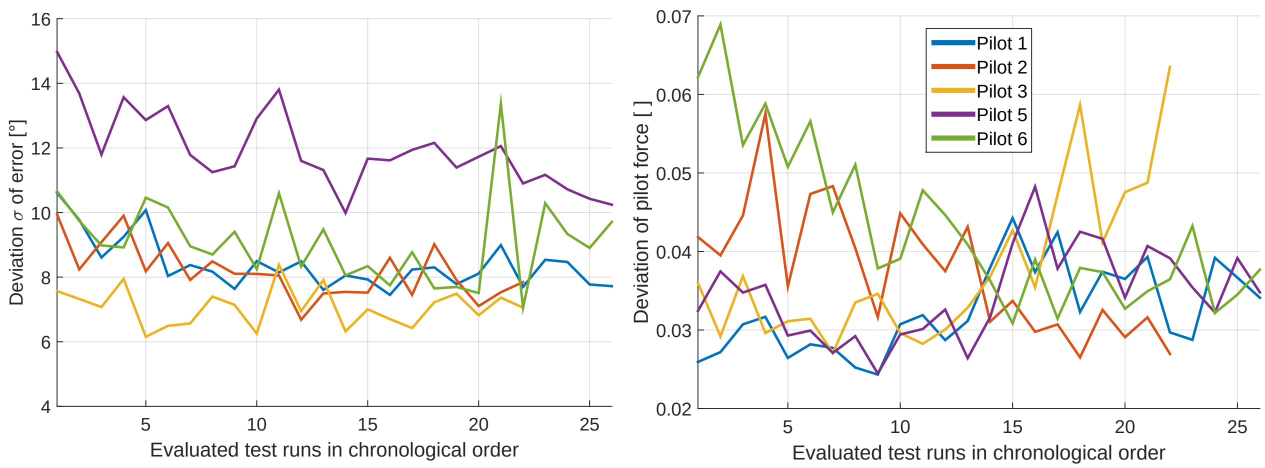

Figure 7. Chronological representation of error deviation (left) and physical workload (right)

Time shifts between pitch attitude and reference function was very different among pilots. In the case of Pilot 3 it was around 0.3 seconds. For Pilot 5 it was longest, around 0.6 seconds. This was due to the flight experience of Pilot 3 and the tiredness that afflicted Pilot 5 from the beginning. Test runs 23 and 26, which were flown entirely with k_3 have high average time shifts. This indicates, that stiffer sidesticks slowed down the pilot inputs.

Based on the analysis of bandwidth and the previous results, Pilots 3 and 5 can be identified as high gain pilots (fast inputs, often with high amplitudes, reacting to high frequent components of the reference function), Pilots 1 and 4 as low gainers and Pilot 2 inbetween. The more aggressive pilots were, the more they preferred a lower force-deflection gradient. Comparison of chronological data leads to the conclusion that the first seven test runs were influenced by adaption. Performances were stable during the second block, although pilots comented that fatigue started to play a role in the last seven runs.

Some pilots tried in vane to descipher the pattern behind the reference function. They could not recognise a pattern in the transitions either. They commented that only the imminent reverse of the flight director bar once it surpassed 25° was predictable.

B. Reactions to force-deflection gradient transitions

In some test runs the pilot reaction to a force-deflection gradient transition, happened as predicted in Figure 1. The effects of increasing and decreasing gradient are depicted in Figure 8. For better visibility, the force-deflection gradient is augmented ten times, the dimensionless stick input 50 times and the transition moment is highlighted by a red dashed line. The left plot is from test run number 54 from Pilot 5. At 25.2 seconds a force-deflection gradient reduction from k_3 to k_1 is commanded in the simulation. After two time steps, or 0.04 seconds later, the torque motors react. The deflection increase between 25.24 and 25.36 seconds corresponds to 1.18° or 22% of the sidestick's forward travel. This unintended additional pitch-up command is the reason for confusion and a larger-than-intended negative pitch rate. To counteract, the pilot almost instinctively pulls the sidestick without adapting his force input at 25.6 seconds all the way to neutral and overreacts. At this moment the error is already zero, but the pilot seems to intend to correct his previous overreaction and pushes the stick forward at 25.9 seconds.

The opposite case is depicted on the right plot of Figure 8. This is the transition from k_1 to k_3 of test run 32 flown again by Pilot 1 at 74.9 seconds. 0.04 seconds later the command arrives at the sidestick. With the current rearward input force but with the new gradient, the torque motors push the sidestick together with the pilot's arm forwardswards in 0.12 seconds. The result are erratic inputs in the following moments.

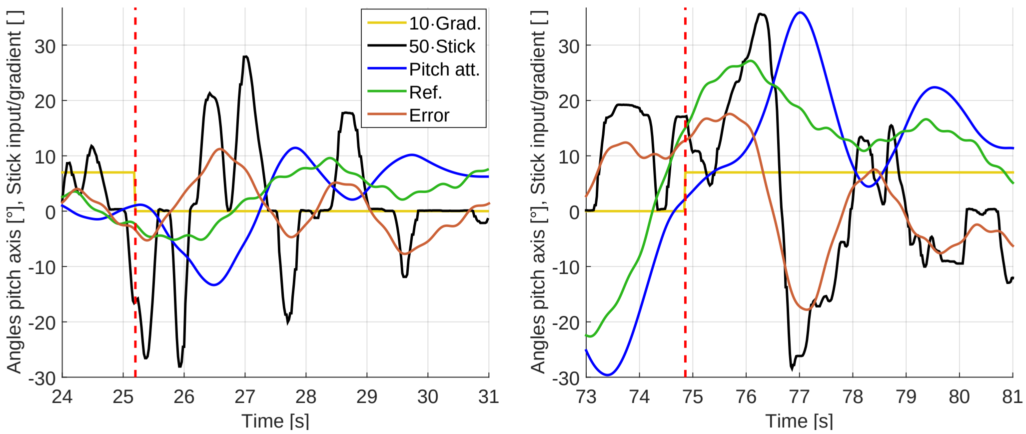

Figure 8. Stick deflection due to decreasing (left) and increasing (right) stick gradient

There were many other examples of surprise reactions. Sometimes the pilots commented that they had felt a disruption, but in many other, with clearly visible leaps of the stick due to the transition, they said not having felt anything. There are two possible explanations: they did not notice, which, given the intense tracking task, seems plausible. Or they were not aware, that an anomaly they might have felt during the run was actually asked for. This is the drawback of not providing details on the transition: the pilot ignores how transitions manifest themseves. The purpose is for the pilot to describe his unbiased experienced.

C. Pilot in-the-loop oscillations

All five pilots encountered PIO's. Most of them during normal tracking but some also due to force-deflection gradient transitions. The analysis presented here will focus solely on the latter. Figure 8 shows how after a transition the attempt to regain control or resume tracking, sometimes paired with the pilot's force misadaption, triggers a PIO. Two PIO-cycles of three seconds duration in Figure 8 (left) and 1.5 cycles on the right.

PIO-suspicious segments were identified manually. But to confirm a PIO, criteria, based on definitions in [14] were established:

- Control inputs of at least 50% of the maximum stick deflection attained during the test run,
- The pitch angle error exceeding 5°. For evaluated runs with overall less error and pilot activity, oscillations with smaller error were considered as a PIO.
- Phase delay of at least 180° of pitch attitude with respect to stick input,

Pilot inputs seldom had well defined extrema to use as reference to compute phase delays, as in Figure 8 (left) at 26.5 seconds. Instead, zero amplitude crossings were used as reference. This approach has to consider that when tracking the reference function, pitch attitude and pilot inputs are not centered around a constantvalue, as would happen when trying to stabilise in horizontal flight. An algorithm capable of measuring phase delay under these conditions was programmed and applied to potential PIO's which already fulfilled the first two criteria. Close examination of the suspected time series had to confirm that the inputs originated as response to aircraft pitch oscillation and not as attempts to track mid-sized waves of the reference function. Even in a PIO, the pilot noticed large peaks of the reference function. They large and continued inputs that they elicited often terminated an oscillation.

A PIO-cycle was defined as a period of ongoinng PIO. The minimal length to reliably determine phase lags was 1.5 cycles and therefore this is the minimum PIO's duration. Table 8 classifies only the PIO's that were triggered by force-gradient transitions. Based on average cycle durations, 3.5 cycles lasted longer than 5 seconds, which was arbitrarily determined as long enough to constitute a violent event and were classified as sustained PIO's. The last row of Table 8 counts PIO's that started by the meachanism of unwanted stick deflections from Figures 1 and 8.

Name	T+3	T+2	T+1	T-1	T-2	T-3
Tot. Cycles	4	-	1.5	-	8	22
Tot PIO's	2	-	1	-	3	10
Sust. PIO's	-	-	-	-	1	1
Defl. PIO's	1	-	1	-	-	8

Table 8. Classification of transition-triggered PIO's

Most of the events (82% of PIO's) happened after the two strongest transitions with decreasing gradient, T-2 and T-3. T-3 was responsible for 8 out of 10 PIO's that originated by unwanted deflections. As the transition occurred in total 30 times, it originated a PIO on 27% of its appearances. Transition T+3 caused two PIO's. This indicates that the gradient increase and initial reduced control authority also caused sufficient confusion that led to a PIO. The central transitions with lower open-loop factors only caused one short PIO.

Figure 9 depicts the duration of the 16 transition-caused PIO's from Table 8, the test run and dynamic during which they happened. The dashed black line deleimits both blocks.

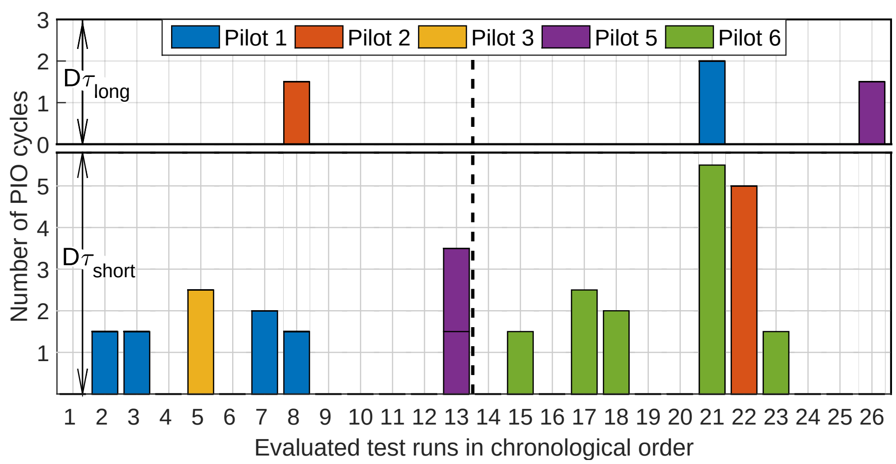

Figure 9. Chronological appearance of transition-caused PIO's by dynamic and pilot

Except for the four first PIO's from Pilot 1, pilots showed signs of good adaptation when they happened: during test runs with $D_{\tau_{short}}$ (13 out 16), mostly in the second half of a block or a test session. This is the case of the last transition-caused PIO encountered by Pilot 1. Pilot 2 encounters PIO's in the second half of both blocks. Although the transition-caused PIO of Pilot 3 happens already at his fifth run, from all the 122 runs, this one has the leas error and indicates good performance. Pilot 5 encountered three PIO's in the last run of both blocks. As explinained before, the first block with $D_{\tau_{long}}$ helped Pilot 6 to quickliy adapt to dynamic $D_{\tau_{short}}$. This explains the high number of transition-triggered PIO's during the second block. These figures make a good case that pilot adaption often favours transition-caused PIO's.

The relation between adaption and transition-caused PIO's is used to detect this kind of transitions without the need to manually analyse the time series. The approach consists of two steps. The first is computing the error deviation in the period between two transitions or a transition and the test run end. Another error deviation for the same period but starting five seconds after the transition is computed. When compared, a considerable difference between them, here set at 1°, indicates a large error during the first five seconds after the transition. 24 transitions were thus detected.

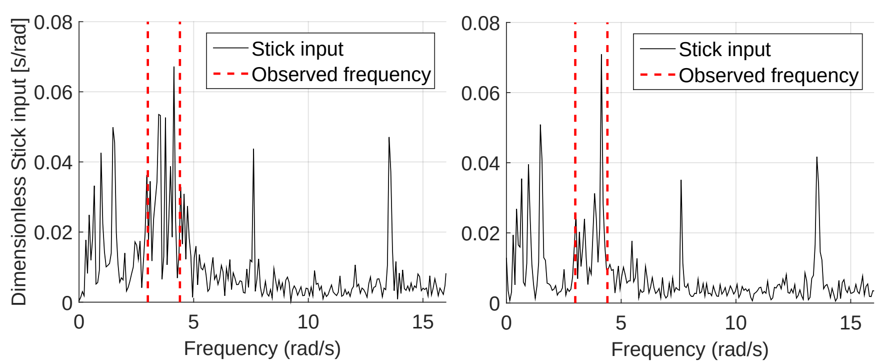

Figure 10. PSD's of Pilot 3. Test Run 32 (not adapted, left) and 51 (adapted, right)

The second step consists in identifying those test runs from the first step, with characteristic PSD's. It was observed, that the PSD of test runs with good pilot adaption showed very few and well defined peaks between 3 and 4.4 rad/s. These frequencies are similar to those at which PIO's occurred. When the pilot was well adapted, the energy content of his inputs concentrated on individual frequencies. When the pilot was not adapted, the energy content between 3 and 4.4 rad/s was more constant and at a relatively high level, without defined peaks. Figure 10 exemplifies the evolution for Pilot 3. Test runs 32 and 55 were respectively his fourth and twentieth.

With the PSD's, 14 of the 24 events found in the first step were excluded as not being transition-triggered. Six PIO's were confirmed as being triggered by a transition. They are among the PIO's in Table 8. The approach did to confirm two cases and falsely indicated a PIO in two more, where time series evidenced an incipient PIO.

VI. Conclusions

A methodology to determine the impact of force-deflection gradient transitions on longitudinal PVS dynamics in simulator tests was developed. It was focused on the investigation of PIO's that resulted from transitions between three force-deflection gradients. The methodology describes the setup of pilot briefings and tracking tasks to make the gradient transition unpredictable for the pilot. This was achieved by combining different reference functions, transition moments and randomisation of the test run sequence and preprogramming of the force-deflection transitions so they activate without external intervention.

The methodology was afterwards verified with five pilots in simulator tests with an active sidestick. The obtained data and pilot comments were evaluated to demonstrate the success of the methodology and approaches to analyse the data and detect PIO's. Pilots commented that the transitions, although expected, sometimes caught them off guard even in the last runs. The pilots had no previous flight test experience and therefore very heterogenous techniques. Parameters calculated with the data were used to determine their aggressiveness and adaption. PIO's caused by gradient transitions were much more common with the more benign aircraft dynamic of the two, when pilots were better adapted and at transitions with large decreasing gradient.

In further steps the methodology is to be verified with test pilots. For this test campaign, reference function and aircraft dynamics should be modified to reduce PIO-tendency during tracking. The test campaign will also allow the integration of rating scales into the process to assess PIO-tendency and severity more acurately. Results from this test campaign will also be used to further refine the criteria to detect transition-caused PIO's without examining the time series.

References

[1] Hegg, J. W., Smith, M. P., Yount, L., and Todd, J., "Features of Active Sidestick Controllers," 13th DASC, AIAA/IEEE, 1994, pp. 31–34.

[2] Li, X., Li, B., and Liu, H., "Discussion on the Application of Active Side Stick on Civil Aircraft," Springer, Cham, 2018, pp. 441–449.

[3] Anonymous, "Final Report on the Accident of the Falcon 900B registered SX-ECH," Tech. Rep. 711, Romania Ministry of Civil Aviation Inspectorate.

[4] Gibson, J. and Hess, R., "Stick Feel System Design," Tech. Rep. AGARD-AG-332, Advisory Group for Aerospace Research and Development, 1997.

[5] Mitchell, D. G., Aponso, B. L., and Klyde, D. H., "Effects of Cockpit Lateral Stick Characteristics on Handling Qualities and Pilot Dynamics," Tech. Rep. CR-4443, NASA, 1992.

[6] Schönfeld, A., "Investigation of Manual Control Behaviour during Flight Control Mode Switching: Test Procedure and Preliminary Results," *2nd CEAS Specialist Conference on Guidance, Navigation and Control*, 2013.

[7] Field, E. J., Rossitto, K. F., and Mitchell, D. G., "Landing Approach Flying Qualities Criteria for Active Transport Aircraft," No. ADP011128, RTO AVT Symposium, 2001.

[8] Mitchell, D. G., Hoh, R. H., Aponso, B. L., and Klyde, D. H., "Proposed Incorporation of Mission-Oriented Flying Qualities to MIL-STD-1797A," Tech. Rep. WL-TR-94-3162, Systems Technology, Inc., Hoh Aeronautics, Inc., 1994.

[9] Gibson, J. C., "Piloted Handling Qualities Design Criteria for High Order Flight Control Systems," Tech. Rep. AGARD-CP-333, 1982.

[10] Schofield, B. L., Twisdale, T. R., Kitto, D. W. G., and Ashurst, T. A., "Development of Handling Qualities Testing in the 70's: A new Direction," Tech. Rep. AGARD-CP-333, Advisory Group for Aerospace Research and Development.

[11] Mooij, H. A., *Criteria for Low-Speed Longitudinal Handling Qualities of Transport Aircraft with Closed-Loop Flight Control Systems*, Doctor thesis, Delft University of Technology, 1984.

[12] Neal, T. P. and Smith, R. E., "An In-Flight Investigation to develop Control System Design Criteria for Fighter Airplanes," Tech. Rep. AFFDL-TR-70-74, Air Force Flight Dynamics Laboratory, 1970.

[13] Damveld, H. J., Beerens, G. C., van Paassen, M. M., and Mulder, M., "Design of Forcing Functions for the Identification of Human Control Behaviour," *Journal of Guidance, Control and Dynamics*, , No. 33, 2010, pp. 1064–1081.

[14] Mitchell, D. G. and Klyde, D. H., "Reccomended Practices for Exposing Pilot-Induced Oscillations or Tendencies in the Development Process," *USAF Developmental Test and Evaluation Summit*, 2004.